THE ASTROPHYSICAL JOURNAL, 561:1016–1026, 2001 November 10

THE AMPLITUDE OF THE KILOHERTZ QUASI-PERIODIC OSCILLATIONS IN 4U 1728−34, 4U 1608−52, AND AQUILA X-1, AS A FUNCTION OF X-RAY INTENSITY

MARIANO MÉNDEZ,[1,2] MICHIEL VAN DER KLIS, AND ERIC C. FORD
Astronomical Institute "Anton Pannekoek," University of Amsterdam and Center for High-Energy Astrophysics, Kruislaan 403, NL-1098 SJ Amsterdam, Netherlands
Received 2000 June 16; accepted 2001 July 25

ABSTRACT

We study the kilohertz quasi-periodic oscillations (kHz QPOs) in the low-mass X-ray binaries 4U 1728−34, 4U 1608−52, and Aql X-1. Each source traces out a set of nearly parallel tracks in a frequency versus X-ray count rate diagram. We find that between two of these tracks, for similar QPO frequency, the 2–60 keV source count rate can differ by up to a factor of ∼4, whereas at the same time the rms amplitude of the kHz QPOs is only a factor of ∼1.1 different. We also find that, for 4U 1608−52 and Aql X-1, the rms spectrum of the kHz QPOs does not depend upon which track the source occupies in the frequency versus X-ray count rate diagram. Our results for 4U 1728−34, 4U 1608−52, and Aql X-1 are inconsistent with simple "extra source of X-rays" scenarios for the parallel tracks, such as those in which the properties of the kHz QPOs are determined only by the mass accretion rate through the disk, whereas X-ray count rate also depends upon other sources of energy that do not affect the QPOs.

Subject headings: accretion, accretion disks — stars: individual (4U 1608−52, 4U 1728−34, Aquila X-1) — stars: neutron — X-rays: stars

1. INTRODUCTION

It is thought that the kilohertz quasi-periodic oscillations (kHz QPOs) in low-mass X-ray binaries reflect the motion of matter in orbit at some preferred radius in the accretion disk around the neutron star (Miller, Lamb, & Psaltis 1998; Stella & Vietri 1999; Osherovich & Titarchuk 1999; Cui 2000; Campana 2000). In most sources, two simultaneous kHz QPOs have been detected, with frequencies between 300 and 1300 Hz. In a given source, the frequency of the QPOs can shift by a few hundred Hz, apparently as a function of $\dot{M}$, the rate at which mass is accreted onto the neutron star (Miller et al. 1998). Yet, it is well known that the relation between the kHz QPO frequencies and X-ray count rate (or X-ray flux), which is assumed to be a good indicator of $\dot{M}$, is complex (Ford et al. 1997a; Zhang et al. 1998; Méndez et al. 1999). In a frequency versus intensity (ν-I_X) diagram a source displays a set of almost parallel tracks. On timescales of a day or less the source moves along one of these tracks with QPO frequency and X-ray count rate positively correlated, whereas on long timescales, in observations separated by a few days the source occupies different tracks in this diagram (see, e.g., Fig. 2 in Méndez et al. 1999).

On timescales of a few days, QPO frequency correlates much better with the X-ray spectral properties of the source than with count rate. In 4U 0614+09 it was found that the frequencies of the kHz QPOs correlate better to the flux of the soft ("blackbody") component in the energy spectrum than to the total X-ray flux (Ford et al. 1997b), whereas a good correlation of QPO frequency with photon index of the power-law component in the energy spectrum has been found in 4U 0614+09 and 4U 1608−52 (Kaaret et al. 1998). The frequencies of the kHz QPOs also correlate much better with the position of the source in an X-ray color-color diagram than with count rate (Wijnands et al. 1997, 1998a; Jonker et al. 1998; Méndez et al. 1999; Méndez & van der Klis 1999; Kaaret et al. 1999a; Méndez 2000; Reig et al. 2000; van Straaten et al. 2000; Di Salvo et al. 2001). This correlation extends to other timing properties as well. The power spectra of these sources often show a broadband noise component that is roughly flat below a break frequency at $\nu_b \sim 1$–10 Hz and decreases above ν_b, and a low-frequency QPO at ∼10–50 Hz. Studies with *EXOSAT* and *Ginga* already demonstrated that the rms amplitude and break frequency of the broadband noise component, and the frequency and rms amplitude of the low-frequency QPO depend monotonically upon the position of the source on the color-color diagram, and correlate much better to colors than to count rate (see van der Klis 1995 for a review). Studies with the *Rossi X-ray Timing Explorer* (*RXTE*) confirmed this across a much wider range of sources (Wijnands et al. 1997, 1998a, 1998b; Jonker et al. 1998, 2000; Markwardt, Strohmayer, & Swank 1999; Boirin et al. 2000; Di Salvo et al. 2001; Bloser et al. 2000) and also showed that both ν_b and the frequency of the low-frequency QPO are strongly correlated to the frequency of the kHz QPOs (Stella & Vietri 1998; Ford & van der Klis 1998; Psaltis, Belloni, & van der Klis 1999; Di Salvo et al. 2001) and to each other (Wijnands & van der Klis 1999).

These correlations have reinforced the idea (Hasinger & van der Klis 1989) that there is one single parameter, inferred to be $\dot{M}$, that governs all the timing and spectral properties of these sources; X-ray flux, which can change more or less independently of the other parameters, is the exception (see also van der Klis et al. 1990; Méndez et al. 1999).

In principle, the disparate behavior of X-ray flux and $\dot{M}$ could be understood if mass flows onto the neutron star through two independent channels (e.g., Ghosh & Lamb 1979; Fortner, Lamb, & Miller 1989). Part of the mass acc-

[1] Also Facultad de Ciencias Astronómicas y Geofísicas, Universidad Nacional de La Plata, Paseo del Bosque S/N, 1900 La Plata, Argentina.
[2] Present address: SRON, Laboratory for Space Research, Sorbonnelaan 2, NL-3584 CA Utrecht, Netherlands.

retion onto the star comes from the disk flow, $\dot{M}_D$, whereas the rest of the mass flux onto the star comes from a radial flow, $\dot{M}_R$. The timing and spectral properties are governed by $\dot{M}_D$, whereas the X-ray luminosity is proportional to $\dot{M}_D + \dot{M}_R$ (Wijnands et al. 1996; Kaaret et al. 1998; Méndez et al. 1999). In this scenario, the frequencies of the kHz QPOs are linked to $\dot{M}_D$, but because $\dot{M}_D$ and $\dot{M}_R$ can vary more or less independently, and both contribute to the total luminosity ($L_D + L_R$), the source traces out separate tracks in the ν-I_X diagram. (The argument is more general, and is still valid if L_R is produced by another source of energy, not necessarily related to a mass inflow.) None of the kHz QPO models so far discussed explicitly predicted the existence of the parallel track phenomenon, and there are therefore no specific predictions for how QPO amplitude varies across tracks. For this reason in this paper we use as a reference the simplest possible scenario, namely, one in which the additional source of energy that produces the extra luminosity producing the parallel tracks does not affect the QPO amplitudes at all. In such a scenario, at a constant kHz QPO frequency (i.e., constant $\dot{M}_D$), the rms amplitude of the QPOs should decrease with count rate, as the source moves from one track to another in the ν-I_X diagram.

In this paper we use *RXTE* data to study the rms fractional amplitude of the kHz QPOs on different tracks in the ν-I_X diagram, that is, as a function of count rate for a fixed QPO frequency. In § 2 we describe the observations and results, and in § 3 we discuss the significance of our findings within the scenario previously described.

2. OBSERVATIONS AND RESULTS

We used observations from the Proportional Counter Array (PCA) on board *RXTE* of the kHz QPO sources 4U 1608−52, 4U 1728−34, and Aql X-1. For 4U 1608−52 the data are the same as those in Berger et al. (1996) and Méndez et al. (1998c), except that here we do not use the observation of 1996 March 6 because only photons from a limited energy range were recorded. For 4U 1728−34 we analyzed the same data as described in Strohmayer et al. (1996, 1997), Ford & van der Klis (1998), Méndez & van der Klis (1999), and Di Salvo et al. (2001). For Aql X-1 we analyzed the same observations as used by Zhang et al. (1998), Cui et al. (1998), and Reig et al. (2000). We discarded those observations for which fewer than five detectors of the PCA were on. This means a loss of ∼2%, ∼2%, and ∼11% of the observations of 4U 1728−34, 4U 1608−52, and Aql X-1, respectively. A few X-ray bursts occurred during these observations, but we excluded those parts of the data from the rest of our analysis.

In all these observations data were recorded using the Standard 2 mode, with 16 s time resolution in 129 energy channels, and in all cases another mode with a time resolution of at least 1/4096 s was running in parallel. We used the Standard 2 data to produce background subtracted light curves (using *Pcabackest* v2.1b) for the full energy range of the PCA (nominally 2–60 keV).

For each source we used the high time resolution data to produce power spectra every 64 s, up to a Nyquist frequency of 2048 Hz, with no energy selection. We searched these power spectra for kHz QPOs, at frequencies $\gtrsim$250 Hz. To do this we first produced a dynamic power spectrum of each observation, we identified those power spectra that showed a strong QPO, and we visually measured its frequency, ν_0. If two QPOs were present in a power spectrum, we always picked the one at lower frequencies, because it was generally the most conspicuous one. We fitted those power spectra, in the range $\nu_0 - 100$ Hz to $\nu_0 + 100$ Hz, using a function consisting of a constant plus one Lorentzian. In a few cases in which the QPOs were not significant enough (less than 3 σ, single trial) in the 64 s segments we averaged several contiguous 64 s segments, but always less than 20, to try and measure the QPO. We did not combine more than 20 consecutive power spectra because the QPO frequencies can vary by a few tens of Hz within a few hundred seconds, and these frequency variations result in biased measurements of the QPO frequencies. We discarded those data for which this procedure did not reveal any significant kHz QPO. We note that in this manner we might have discarded data with weak QPOs that could have been detected using more data.

On several occasions we also detected the upper kHz QPO, either directly in the dynamical power spectrum or after we averaged (or shifted and averaged; see below) the power spectra of an observation. In those cases, to increase the significance of this QPO and to facilitate measuring it, we aligned the individual power spectra according to the frequency of the lower QPO, collected them into groups such that the frequency of this QPO did not vary by more than 10–50 Hz, and calculated the average power spectrum for each group (see Méndez et al. 1998b). We fitted these power spectra, in a range of 200 Hz around the approximate frequency of the upper kHz QPO, using a constant plus one Lorentzian.

In those cases in which we detected only one QPO, we analyzed the average power spectrum of that observation to try and identify it as either the lower or the upper kHz QPO. If the average power spectrum still showed a single QPO, we calculated the shifted-and-averaged power spectrum, using the frequency of the QPO we had detected as a reference to shift the individual power spectra. If no other QPO was detected after this procedure (this was the case for all Aql X-1 data; see below) we treated that observation separately, so that in the rest of our analysis the identification of the kHz QPOs as upper or lower is unambiguous.

In Figure 1 we plot the rms fractional amplitude of the QPOs that we detect in each source, as a function of their frequency (see also Di Salvo et al. 2001, Fig. 3*b*). For 4U 1728−34 and 4U 1608−52, when we detect two kHz QPOs simultaneously, we use filled and open circles for the rms amplitude of the lower and the upper kHz QPO, respectively; when we detect only a single QPO we use open squares to plot its rms amplitude. For Aql X-1 we use open squares to plot the rms amplitude of the only kHz QPO so far detected. It is apparent that in 4U 1728−34 and 4U 1608−52 the amplitude of the upper kHz QPO is usually larger than that of the lower kHz QPO, and that the amplitude of the upper kHz QPO decreases monotonically with frequency, whereas the rms amplitude of lower kHz QPO first increases, and then decreases with frequency. When only one QPO is detected in 4U 1728−34 and 4U 1608−52, the rms amplitude of that QPO (*open squares*) is consistent with the relation for the upper kHz QPO in those sources.

Aql X-1 is different from 4U 1608−52 and 4U 1728−34 in that it shows only a single kHz QPO in its power spectrum (Zhang et al. 1998; Cui et al. 1998; Reig et al. 2000).

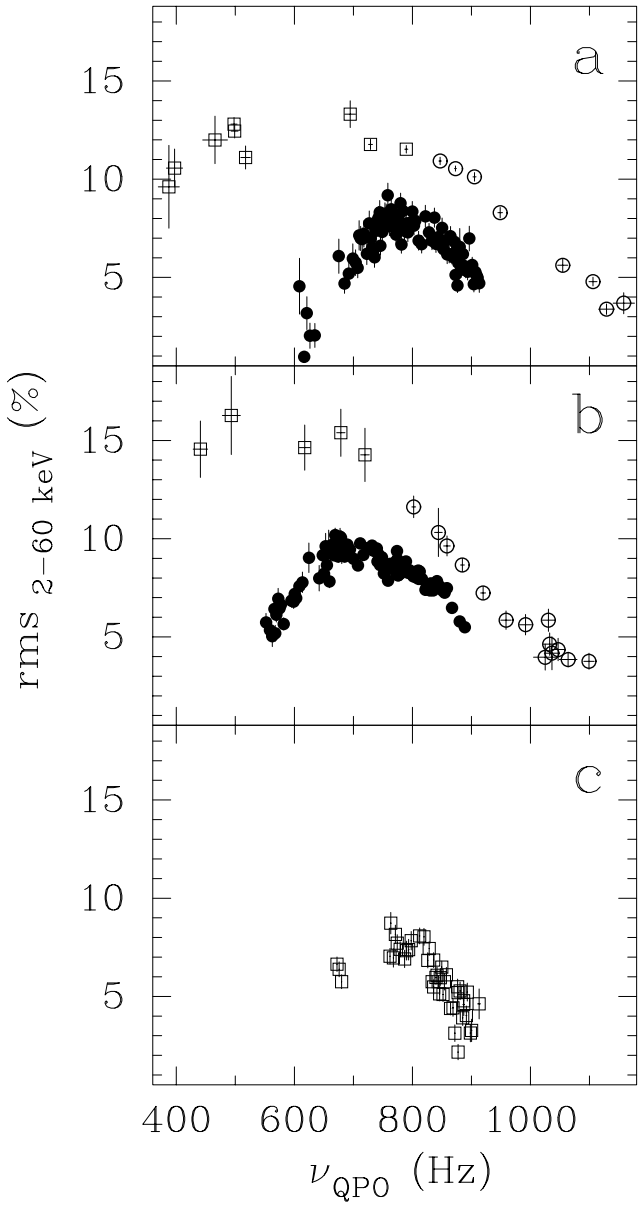

FIG. 1.—Amplitude of the kHz QPOs as a function of their frequency for (*a*) 4U 1728−34, (*b*) 4U 1608−52, and (*c*) Aql X-1. For 4U 1728−34 and 4U 1608−52 the filled and open circles show the relation for the lower and the upper kHz QPO, respectively, and open squares indicate measurements in which we detect only a single QPO. For Aql X-1 the open squares show the relation for the only kHz QPO so far detected. The rms amplitudes are for the full PCA energy band.

We applied the procedure described above to each of the observations of Aql X-1 in which this kHz QPO was detected, but in none of them could we detect a second QPO. Because in Aql X-1 we see only a single kHz QPO, it is difficult to tell whether in all cases it is the same peak, and if so, whether it is the lower or the upper kHz QPO. However, (1) plots of the QPO frequency versus X-ray color (Méndez 2000), or versus position of the source in a color-color diagram (Reig et al. 2000), are consistent with one single relation; (2) the average FWHM of the QPO in Aql X-1 is ∼10 Hz (it goes from ∼2 to ∼20 Hz), similar to the FWHM of the lower kHz QPO (but significantly less than the average FWHM of the upper kHz QPO) in 4U 1728−34, 4U 1608−52, and 4U 1636−53 (Strohmayer et al. 1996; Méndez et al. 1998c; Méndez, van der Klis, & van Paradijs 1998a; Kaaret et al. 1999b); (3) the relation of the rms amplitude of the QPO versus the QPO frequency is similar to that of the lower kHz QPO in 4U 1608−52 and 4U 1728−34 (see Fig. 1); (4) the photon energy spectrum of the kHz QPO in Aql X-1 (see below) is consistent with that of the lower kHz QPO in 4U 1608−52, and significantly different from that of the upper kHz QPO in the same source (Berger et al. 1996; Méndez et al. 1998b). We conclude that whenever a kHz QPO was detected in these observations of Aql X-1, it was always the same one, and we identify it as the lower kHz QPO. In what follows we use all the data with the kHz QPO from this source.

Figure 2 shows, for 4U 1728−34, 4U 1608−52, and Aql X-1, the relation between the frequency of the lower kHz QPO, ν_1, and the 2–60 keV background subtracted count rate. As we explained above, in a few occasions we had to average several consecutive 64 s segments to get a significant measurement of the QPOs, and for that reason each point in this figure represents between 64 (∼63% of the points) and 1280 s of data (only ∼8% represent more than 256 s of data). The figure shows, for each source, the well-known parallel tracks in the ν-I_X diagram (e.g., Ford et al. 1997b; Méndez et al. 1999).

For each source, we measured the rms fractional amplitude of the lower and the upper kHz QPO, at constant QPO frequencies, as a function of count rate. For this purpose we grouped the power spectra according to the frequency of the lower QPO (Fig. 2), such that ν_1 did not vary by more than ∼40 Hz in each frequency range. For every source, we averaged the power spectra in each frequency range on each of the more or less parallel tracks in Figure 2. For every frequency and count rate interval, the average power spectrum was calculated by first aligning the individual power spectra according to the frequency of the lower QPO displayed in Figure 2. In this way, if there was a second QPO in the power spectra, it would become more significant after the alignment, and would be easier to measure its properties (see Méndez 2001).

We fitted each of these average power spectra (one per frequency interval and per track for each source) using a constant plus one or two Lorentzians. The errors in the fit parameters were calculated using $\Delta\chi^2 = 1$ (1 σ for a single parameter). For 4U 1608−52 and 4U 1728−34, when the upper QPO was not significant, we fixed its frequency to $\nu_1 + \Delta\nu$, with $\Delta\nu$ determined from Figure 3 of Méndez et al. (1998c) and Figure 1 of Méndez & van der Klis (1999), respectively, and we calculated upper limits to its amplitude using $\Delta\chi^2 = 2.71$, corresponding to a 95% confidence level.

Figures 3 and 4 show the rms amplitude of the lower and the upper kHz QPOs as a function of count rate, for different frequency intervals in 4U 1728−34 and 4U 1608−52, respectively; similarly, Figure 5 shows the rms amplitude of the only kHz QPO in Aql X-1. Each panel in those figures presents data for the indicated frequency interval; each point belongs to an individual track in Figure 2. From these figures it is apparent that, for a fixed QPO frequency, the source count rate can increase by up to a factor of ∼4, but the rms fractional amplitude decreases only by a factor of ∼1.1. There are 13 cases for which the rms is consistent with being constant and nine cases in which it decreases with count rate.

Assuming that a fraction ξ of the X-ray count rate I_D produced by the disk mass inflow $\dot{M}_D$ is modulated, the

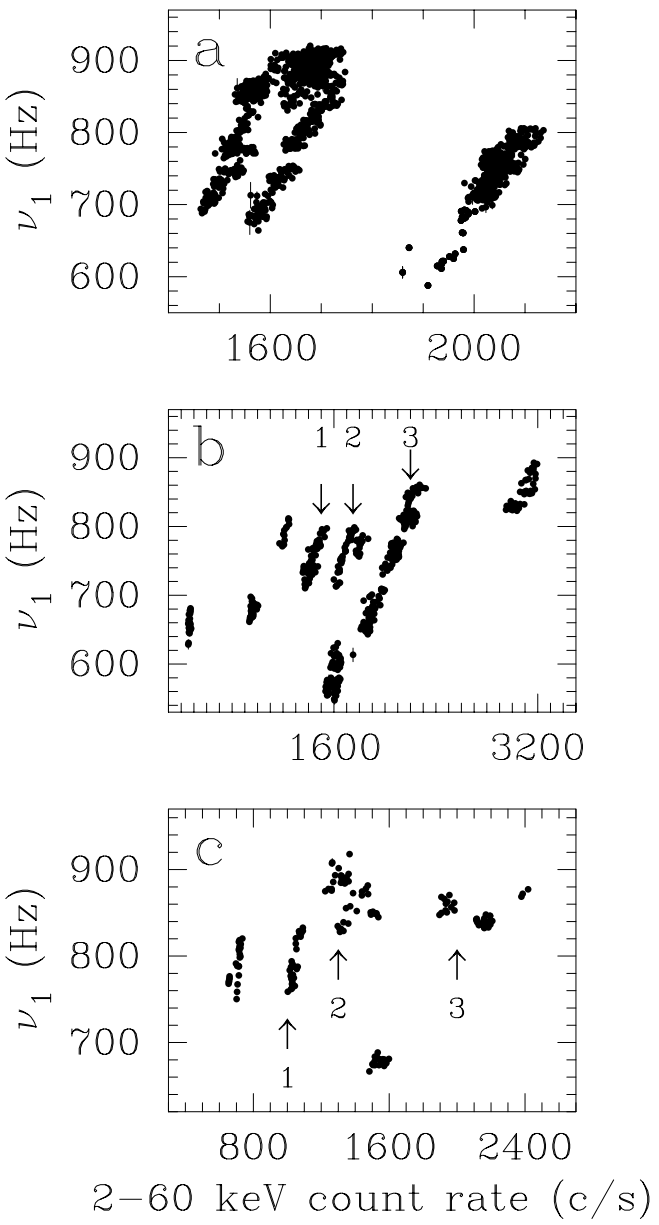

FIG. 2.—Frequency of the lower kHz QPO vs. the 2–60 keV count rate for (*a*) 4U 1728−34, (*b*) 4U 1608−52, and (*c*) Aql X-1. The count rates have been corrected for background, and are for five detectors. For 4U 1728−34 and 4U 1608−52 we include only data where both kHz QPOs were detected simultaneously, so we can unambiguously identify the lower kHz peak. For Aql X-1 we plot the only kHz QPO detected in the power spectrum. For 4U 1608−52 and Aql X-1 we indicate three tracks on which we calculate the photon spectrum of the QPO (see text and Fig. 7).

fractional rms amplitude of a QPO can be expressed as $\mathrm{rms} = \xi I_D/(I_D + I_R)$, where I_R is the X-ray count rate produced by $\dot{M}_R$. If all QPO properties are a function of I_D only, at constant QPO frequency the ratio of the QPO rms amplitudes on tracks j and k in the ν-I_X diagram, $\mathrm{rms}_j/\mathrm{rms}_k$, has to be equal to the inverse ratio of count rates in those tracks, $I_{X,k}/I_{X,j}$. Except in the case of the upper kHz QPO in 4U 1608−52 for which only two measurements were available, we fitted a linear relation to the rms amplitude ratio versus the inverse count rate ratio, $\mathrm{rms}_j/\mathrm{rms}_k = aI_{X,k}/I_{X,j} + b$, for each QPO independently. For the lower kHz QPO in 4U 1728−34 we get $a = 0.16 \pm 0.09$ and $b = 0.83 \pm 0.07$, respectively, $\chi^2_\nu = 2$ for 27 degrees of freedom (dof). For the upper kHz QPO in 4U 1728−34, $a = -0.41 \pm 0.41$ and $b = 1.23 \pm 0.36$, respectively, $\chi^2_\nu = 0.9$ for 7 dof. For the lower kHz QPO in 4U 1608−52, $a = 0.25 \pm 0.06$ and $b = 0.75 \pm 0.04$, respectively, $\chi^2_\nu = 5.1$ for 27 dof. For the only kHz QPO in Aql X-1, $a = 0.53 \pm 0.09$ and $b = 0.50 \pm 0.07$, respectively, $\chi^2_\nu = 1.1$ for 20 dof. (Some of the fits are formally unacceptable, which could be due, for instance, to frequency-dependent changes of the QPO rms.) Except for the upper kHz QPO in 4U 1728−34, for which the error bars are too big to draw any conclusion, for all the other QPOs both a and b are significantly different from the expected values, $a = 1$ and $b = 0$.

In Figure 6 we summarize this information. We show the ratio of the kHz QPOs rms amplitude versus the inverse of the corresponding count rate ratio, for points from the individual panels in Figures 3, 4, and 5 (i.e., for a small frequency range of the lower kHz QPO) taken in pairs (we used only data from panels that contain 2 or more points in them). The dashed line in that figure shows the relation expected in simple "extra source of X-rays" scenarios, $\mathrm{rms}_j/\mathrm{rms}_k = I_{X,k}/I_{X,j}$. The solid line indicates the best fit to the data using a straight line, $\mathrm{rms}_j/\mathrm{rms}_k = aI_{X,k}/I_{X,j} + b$. The best-fit parameters are $a = 0.28 \pm 0.04$ and $b = 0.73 \pm 0.03$, respectively (the uncertainties are the 1 σ errors) with a reduced χ^2 of 3 for 92 dof (which indicates that a single line is not a good fit to the data, as might be expected if, for example, there are some source to source changes). We also fitted the data to a constant, which yields a reduced χ^2 of 4.8 for 93 dof. This means an F-test probability of 1×10^{-10} against the hypothesis that the fits using a linear function and a constant are statistically equivalent. In the case of the linear fit, both a and b are significantly different from their expected values. The reduced χ^2 is significantly larger (54 for 94 dof) if we fixed $a = 1$ and $b = 0$.

Finally, we measured the rms energy spectrum of the lower and the upper kHz QPOs in 4U 1608−52, and the only kHz QPO in Aql X-1, when these two sources occupied three different tracks in the ν-I_X diagram (Fig. 2), at constant lower QPO frequency. (Unfortunately, during the 1996 observations of 4U 1728−34—the points that trace out the track at the highest count rate in Figure 2*a*—the high time resolution data contain no energy information, so that it was not possible to do the same analysis for this source.) We divided the data into four energy bands, 2.0–4.6–8.0–13.0–21.5 keV, and calculated the power spectra for both sources in each band. In Figure 7 we show the rms energy spectrum of these QPOs. For 4U 1608−52 we selected data with QPO frequency between 700 Hz and 800 Hz, from tracks 1, 2, and 3 in Figure 2*b*, at ∼1300–1500 counts s^{-1}, ∼1600–1800 counts s^{-1}, and ∼1800–2400 counts s^{-1}, respectively; for Aql X-1 we selected data with QPO frequency between 820 Hz and 860 Hz, from tracks 1, 2, and 3 in Figure 2*c*, at ∼1000 counts s^{-1}, ∼1200–1400 counts s^{-1}, and ∼1800–2200 counts s^{-1}, respectively. For each source, we use different symbols to indicate measurements at each of these tracks (see figure caption). Because in 4U 1608−52 the upper kHz QPO is less significant than the lower kHz QPO, for the upper QPO we measured the rms spectrum using the combined data of tracks 1, 2, and 3. Figure 7 shows that (1) in both sources, the rms energy spectrum of the QPO is independent of the track that the source occupies in the ν-I_X diagram (Fig. 2; notice that the

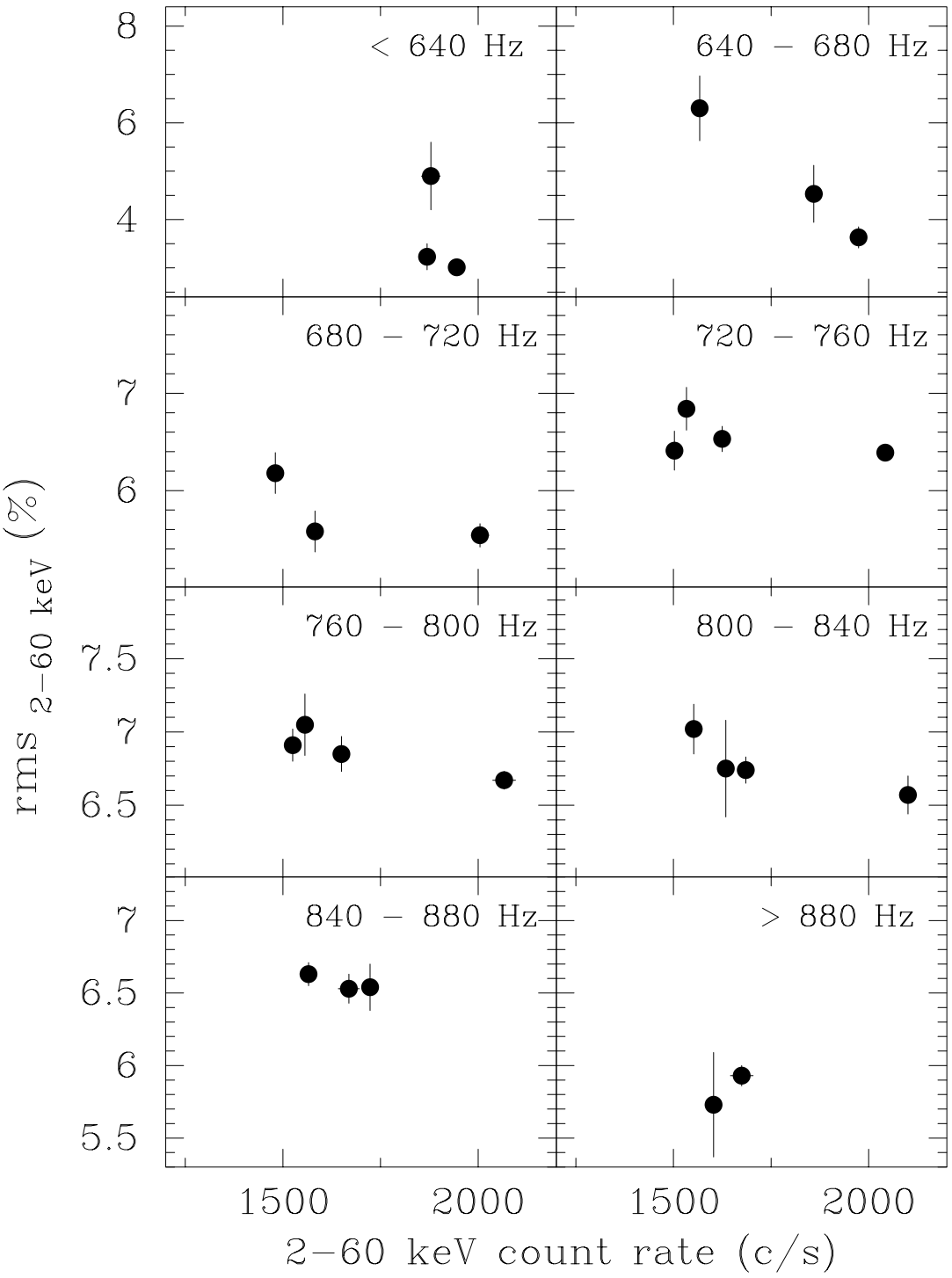

FIG. 3*a*

FIG. 3.—(*a*) Rms amplitude of the lower kHz QPO in 4U 1728 − 34 as a function of the 2–60 source count rate, for different lower QPO frequency intervals as indicated. The rms amplitudes are for the full PCA energy band. (*b*) Same as Fig. 3*a*, for the upper kHz QPO in 4U 1728 − 34.

overall normalization of the rms spectrum decreases as count rate increases, corresponding to the decrease of rms amplitude with count rate shown in Figs. 4 and 5); (2) the rms spectrum of the only kHz QPO in Aql X-1 is similar to that of the lower kHz QPO in 4U 1608−52, but significantly different from that of the upper kHz QPO in 4U 1608−52.

3. DISCUSSION

For 4U 1728−34, 4U 1608−52, and Aql X-1 the frequencies of the kHz QPOs trace several, almost parallel, tracks when plotted versus X-ray count rate (Fig. 2). We measured the rms fractional amplitude of the kHz QPOs in these three sources at different values of the QPO fre-

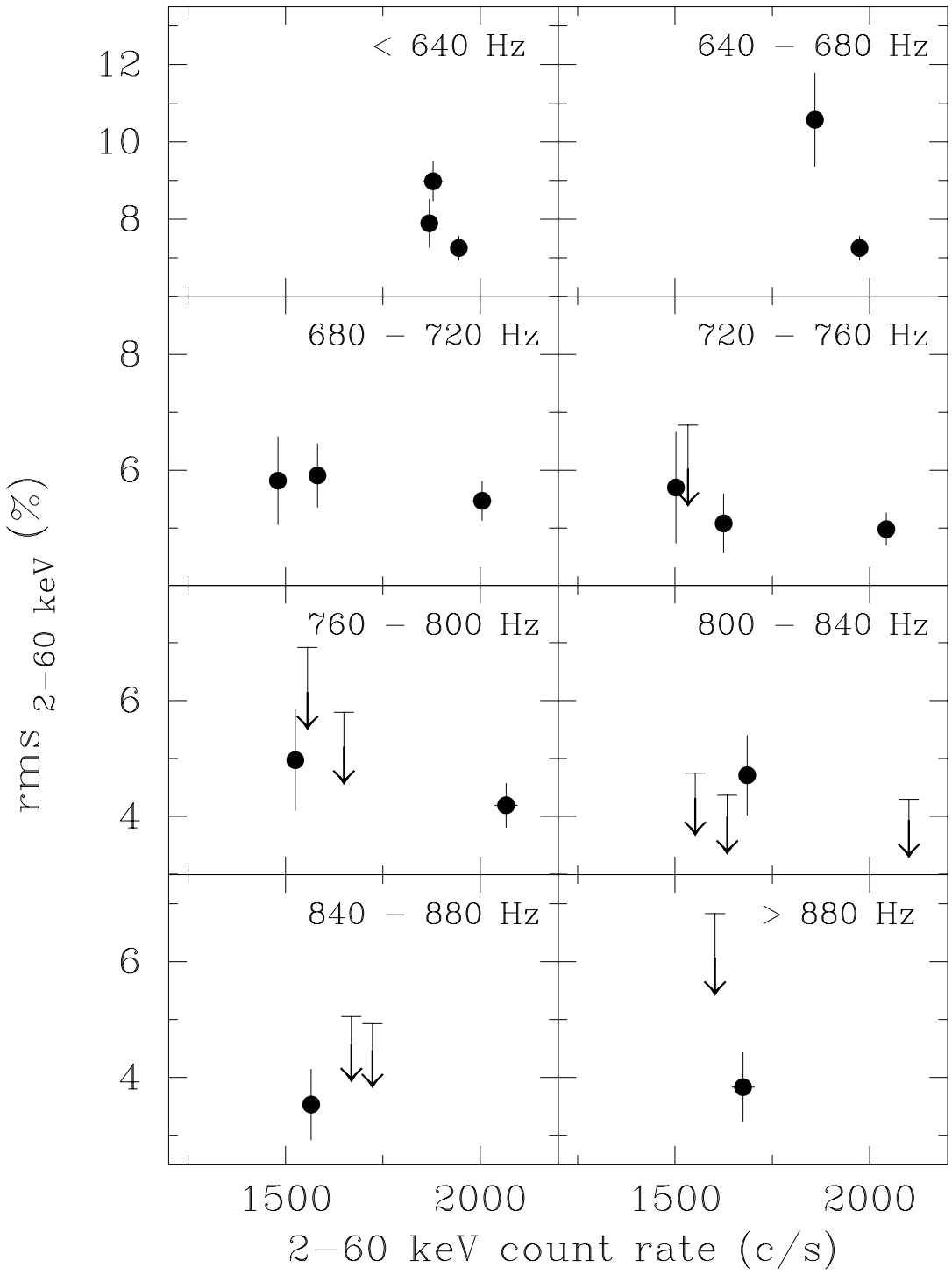

FIG. 3*b*

quency, as a function of count rate. We find that, for a fixed QPO frequency, moving from one track to another in Figure 2, while the count rate increases by up to a factor of ~ 4, the rms fractional amplitude of the QPOs decreases only by a factor of ~ 1.1 (Figs. 3, 4, 5, and 6). This result is inconsistent with simple "extra source of X-rays" scenarios in which the separate tracks in Figure 2 arise from a luminosity component that does not affect the QPO. Furthermore, we also find that the rms spectrum of the lower kHz QPO in 4U 1608−52 and that of the only kHz QPO in Aql X-1 do not depend upon which track the source occupies in Figure 2.

It is well known that the lack of correlation between kHz QPO frequencies and X-ray count rate on timescales longer than a day (Fig. 2) can coexist with a very good correlation between frequency and position in the X-ray color-color diagram (see § 1). It was proposed that this dichotomy could be explained in terms of two independent mass accretion rates, a disk and a radial inflow; while both of them determine the luminosity of the source, only the mass flow

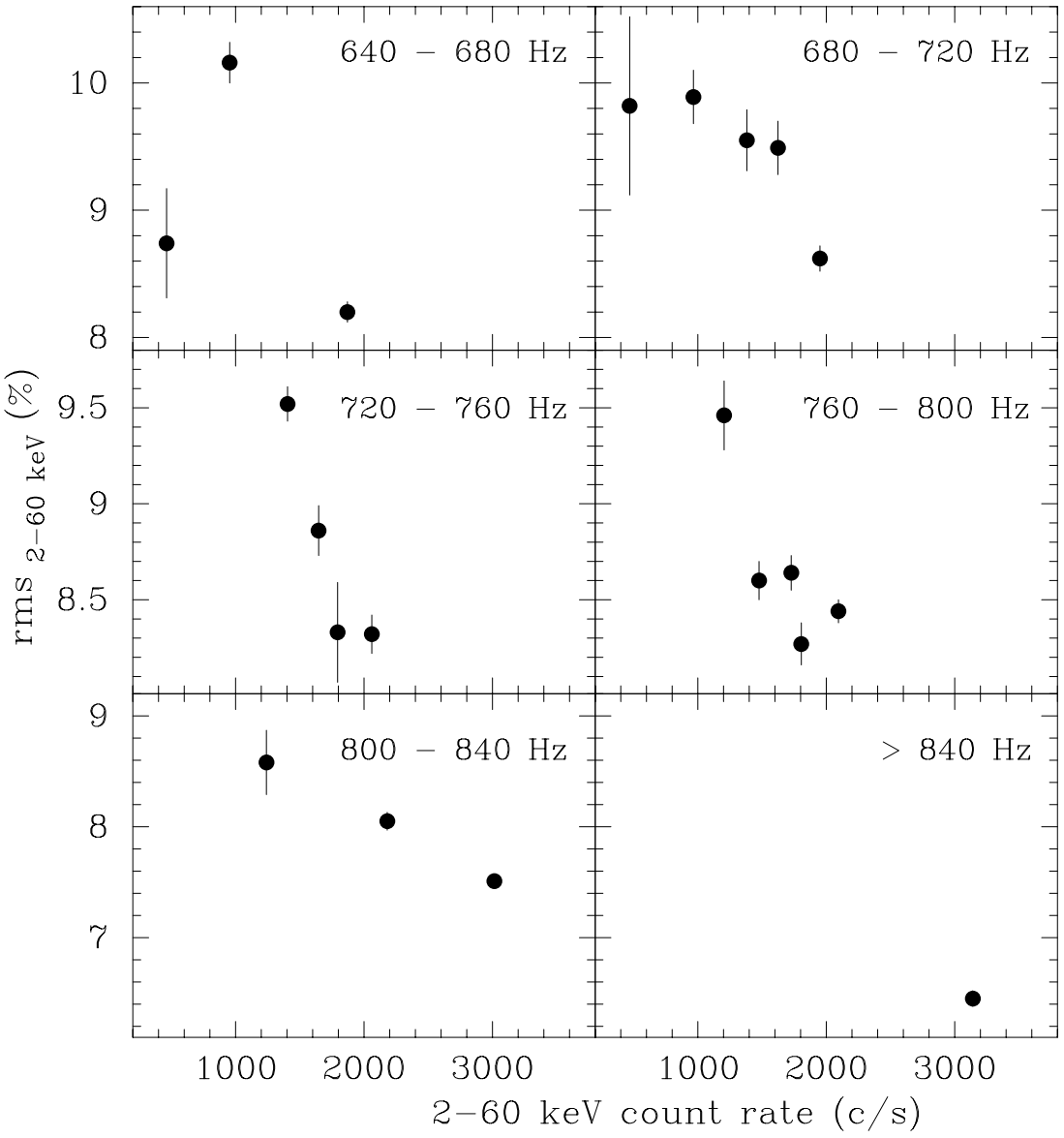

FIG. 4*a*

FIG. 4.—(*a*) Same as Fig. 3*a*, for the lower kHz QPO in 4U 1608 − 52. (*b*) Same as Fig. 3*a*, for the upper kHz QPO in 4U 1608 − 52.

through the disk determines the frequency of the kHz QPOs (Kaaret et al. 1998; Méndez et al. 1999). Our results for 4U 1728−34, 4U 1608−52, and Aql X-1 are inconsistent with version of this scenario where the variations in the radial flow do not appreciably affect the QPO amplitude: the rms fractional amplitudes of the kHz QPOs measured at constant frequency do not decrease rapidly enough as count rate increases (Fig. 6).

The changes in the X-ray intensity may be due to anisotropies in the radiation pattern. It is, however, unlikely that the radiation that is modulated in the kHz QPO mechanism is anisotropic, as kHz QPOs have been observed at roughly similar amplitude in sources spanning a large range of inclinations (e.g., Barret et al. 1997; Homan & van der Klis 2000). Perhaps, there is a large-scale redistribution of some of the emitted energy over unobserved spectral bands. Alternatively, the missing energy might be used to accelerate a jet. While radio emission has been detected from Aql X-1 during X-ray outbursts, and perhaps from 4U 1728−34, it is unlikely that this explanation applies to 4U 1608−52, as no radio emission has ever been detected from this source (Fender & Hendry 2000).

A similar parallel-tracks phenomenon is observed in the ensemble of sources with kHz QPOs (van der Klis 1997; Ford et al. 2000; see also Zhang, Strohmayer, & Swank 1997): While for individual sources, on a timescale of hours, QPO frequency and X-ray luminosity are in general correlation with each other, sources that span more than 2 orders of magnitude in luminosity show kHz QPOs that cover the same range of frequencies. The fractional rms amplitudes of the kHz QPOs are ∼2–20 times larger in the atoll sources, at luminosities of ∼0.005 to ∼0.2 of the Eddington luminosity, than in the *Z* sources, which are near-Eddington, and hence 5–400 times more luminous. For instance, the rms amplitudes of the lower and upper kHz QPO in the *Z* source GX 5−1, which is thought to emit at the Eddington luminosity, are 1%–3% rms and 2%–4% rms, respectively, whereas for the atoll source 4U 0614+09, with a luminosity

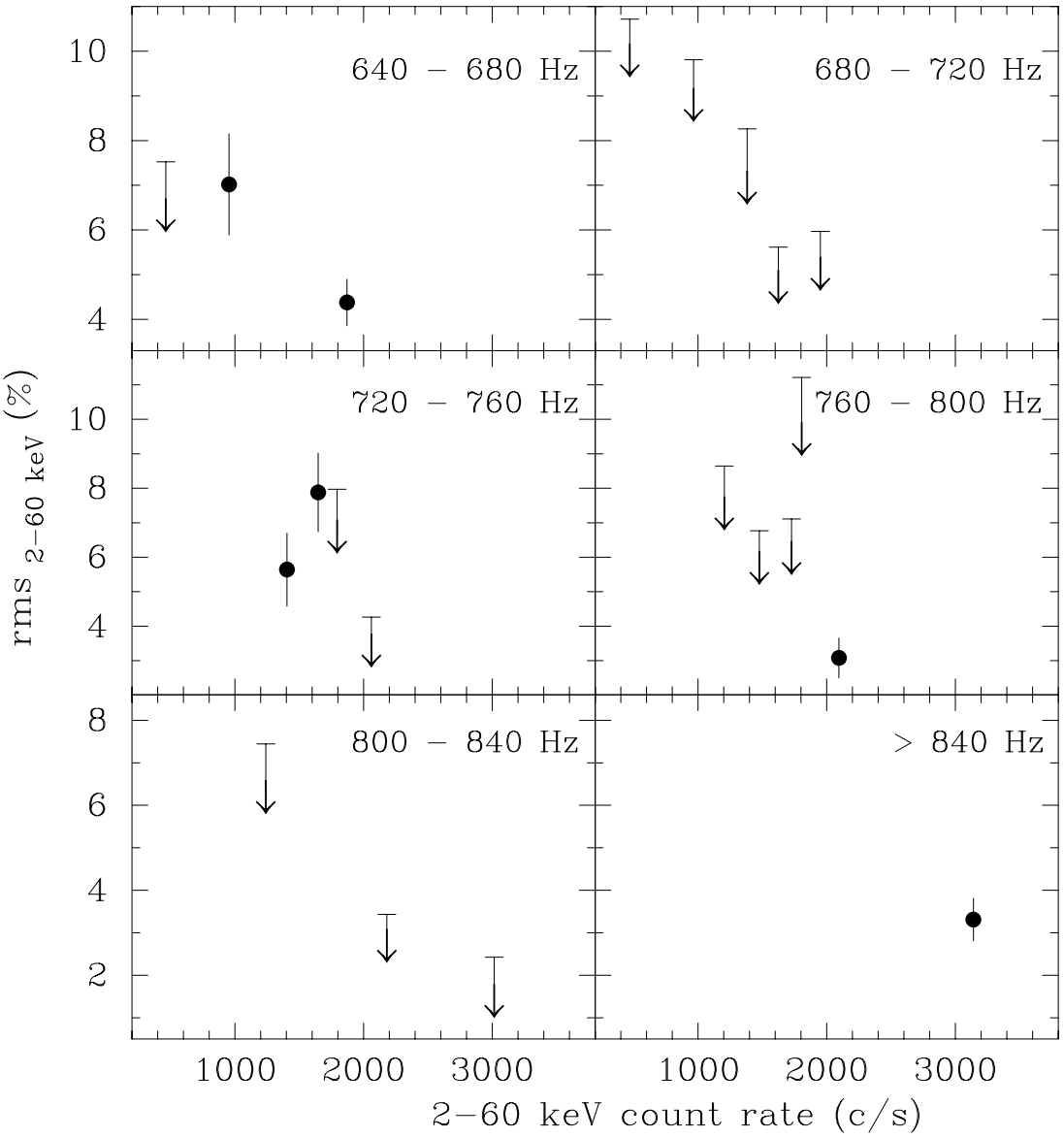

FIG. 4*b*

below ~0.01 of the Eddington luminosity, the amplitudes of the lower and upper kHz QPOs are 6%–25%, and 6%–18%, respectively (Wijnands et al. 1998a; van Straaten et al. 2000; see Hasinger & van der Klis 1989 for a definition of the *Z* and atoll classes). In most cases, the decrease of the fractional rms amplitude of the kHz QPOs in the *Z* sources compared to the atoll sources is less, often by large factors, than the corresponding increase in luminosity which, as in the case of the parallel tracks within individual sources, once again argues against the idea that the difference in luminosity at constant QPO frequency is only due to changes in some luminosity component that does not affect the QPO. However, while there might be a parameter that changes from one source to another to compensate for the dramatic increase in luminosity leaving the QPO frequency unchanged (e.g., the magnetic field strength; White & Zhang 1997), this cannot be the explanation for the discrepancy within individual sources discussed in this paper.

In principle, our results could be explained if the kHz QPO modulates the luminosity from the radial inflow. However, it is unlikely that this is the case. Lee & Miller (1998) have recently suggested that it might be possible for the Comptonizing corona to change the rms amplitude of the kHz QPOs independently of the modulation of the radiation emitted by the disk (see also Miller et al. 1998; Lehr, Wagoner, & Wilms 2000). If this were the case, changes in the properties of the corona in different tracks of the ν-I_X diagram might be the reason for the insufficiently rapid decrease of rms amplitude of the QPOs with count rate (Fig. 6). (Although it is irrelevant to the present issue, we note in passing that some of the conclusions in the paper by Lee & Miller are based on the wrong sign of the QPO phase lags; see Vaughan et al. 1997, 1998).

However, it is known that in 4U 1608−52 (and in several other sources) at fixed QPO frequency, the hard color does not change significantly between different tracks in the ν-I_X diagram (Kaaret et al. 1998; Méndez et al. 1999; Méndez 2000). On the other hand, here we have shown that the rms spectrum of the lower kHz QPO in 4U 1608−52 (and of the only kHz QPO in Aql X-1) does not depend upon the track

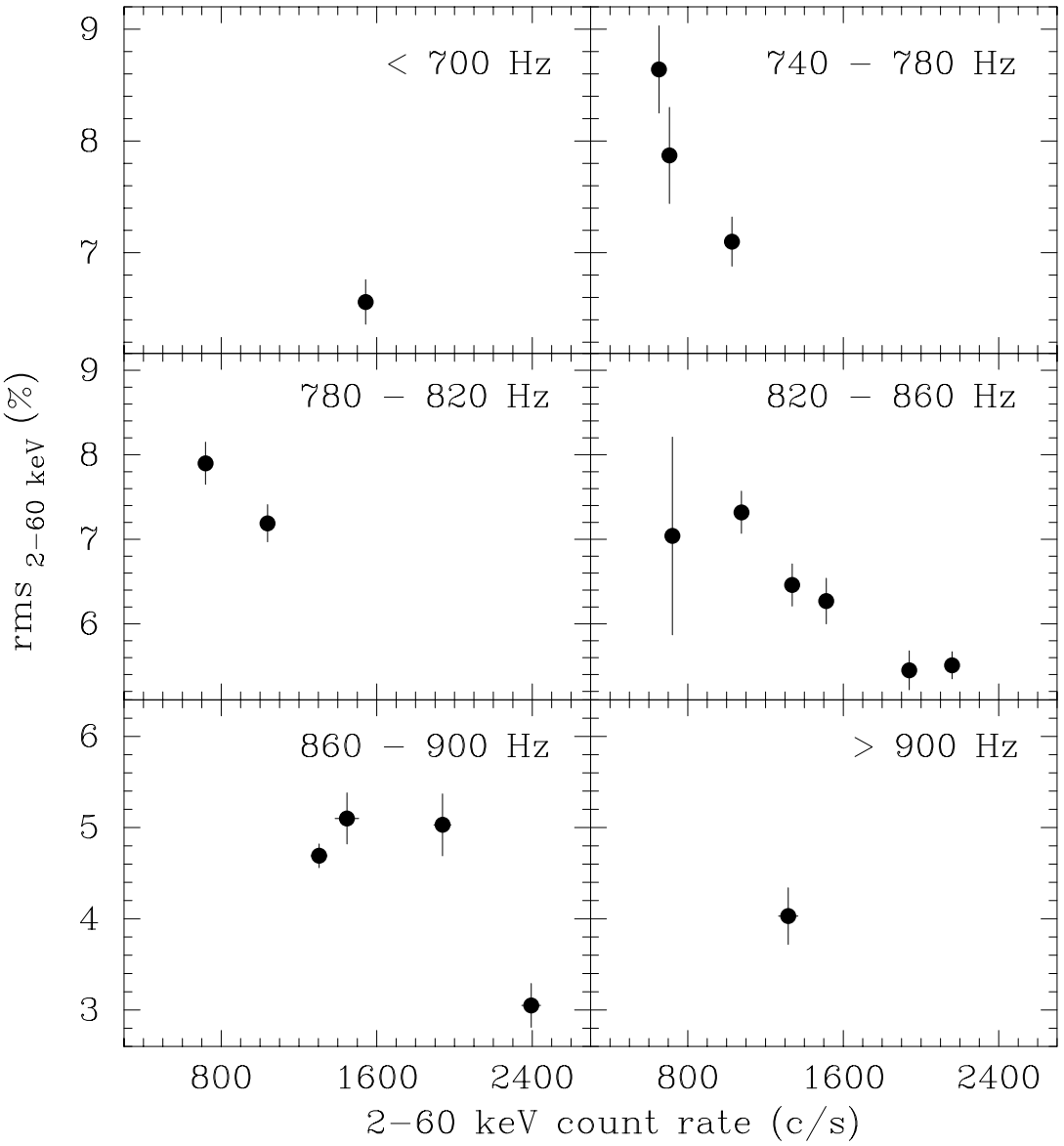

FIG. 5.—Same as Fig. 3*a*, for the only kHz QPO in Aql X-1

that the source occupies in Figure 2. As long as the high-energy part of the X-ray spectrum is produced by inverse Compton scattering in this corona, and the corona is also responsible for the rms spectrum of the kHz QPO, these two results indicate that the properties of the corona do not change significantly from one track to another. This argues against the idea that changes in the properties of the corona could explain the discrepancy between the observed and the expected rate at which the rms amplitude of the kHz QPOs decrease with count rate (Fig. 6).

Our simple scenario does not rule out any of the QPO models so far proposed, for none of these models explicitly predicted the parallel track phenomenon or the behavior of the QPO rms amplitude across the parallel tracks. But given that several of the QPO models are compatible with the simple scenario described in this paper, our results rejecting this scenario can be used to further constrain those QPO models.

Recently, a new mechanism has been proposed that could explain the parallel tracks in the ν-I_X diagram of single sources as well as across the ensemble of sources. Instead of two physical parameters (e.g., $\dot{M}_D$ and $\dot{M}_R$) that vary independently, van der Klis (2001) proposes that source luminosity and kHz QPO frequency are both determined by a single parameter, to which the system has both an instantaneous and a long-term average response. van der Klis (2001) discusses scenarios where this single parameter is the disk accretion rate $\dot{M}_D$, and QPO frequency (set by the inner disk radius) is determined by the ratio of $\dot{M}_D$ to the total luminosity. He shows that he can reproduce the observed parallel tracks and several of their observed characteristics if the long-term average response to $\dot{M}_D$ is, for instance, $\dot{M}_R$, and luminosity depends upon the total mass accretion rate. In models of this type it turns out that QPO frequency depends upon $\dot{M}_D$ normalized by its own long-term average (in our example, $\dot{M}_R$). So, points with the same QPO frequency on different tracks correspond, in this scenario, to source states where both $\dot{M}_D$ and $\dot{M}_R$ are different, but their ratio is the same. The relative strengths of the QPOs in the two cases will depend on the strengths with which they are

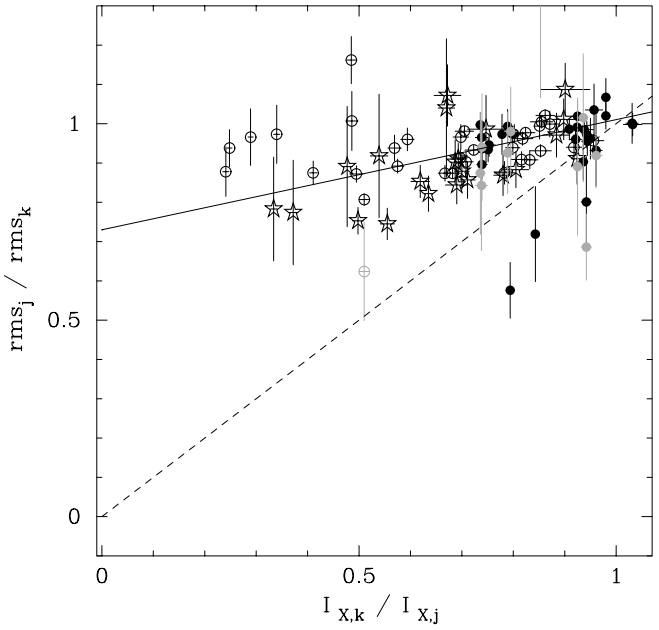

FIG. 6.—Ratio of the kHz QPO rms amplitude vs. the inverse of the corresponding count rate ratio, for each pair of points from the panels with two or more points in Figs. 3, 4, and 5. The lower and upper kHz QPOs in 4U 1728−34 are plotted using black and gray filled circles, respectively. The lower and upper kHz QPOs in 4U 1608−52 are plotted using black and gray open circles, respectively. The kHz QPO in Aql X-1 is plotted using black open stars. The dashed line shows the expected relation for the "extra source of X-rays" scenario with slope 1 and intercept 0 (see text). The solid line is the best-fit straight line to the data, with slope 0.28 ± 0.04 and intercept 0.73 ± 0.03.

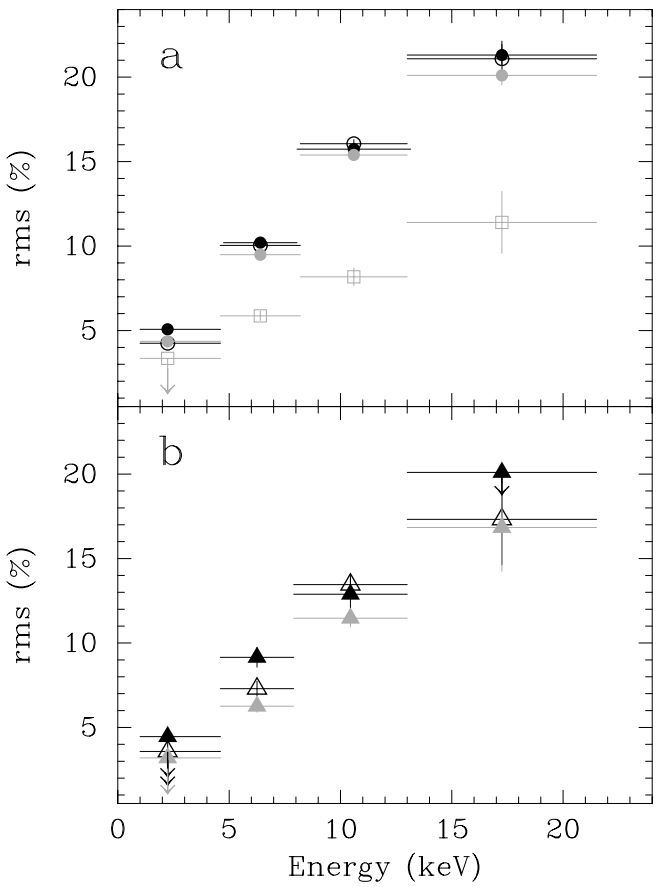

FIG. 7.—Rms energy spectrum of (*a*) the lower and upper kHz QPOs in 4U 1608−52 and (*b*) the only kHz QPO in Aql X-1. For the lower QPO in 4U 1608−52 we use filled black, open black, and filled gray circles to indicate measurements from tracks 1, 2, and 3 in Fig. 2*b*, respectively. We use gray open squares to indicate measurements of the upper kHz QPO in 4U 1608−52. In this case we use the combined data from tracks 1, 2, and 3. For the QPO in Aql X-1 we use filled black, open black, and filled gray triangles to indicate measurements from tracks 1, 2, and 3 in Fig. 2*c*, respectively.

formed (at the same disk radius but under conditions of different accretion rate), and on the propagation effects of the QPO signal through radial flows of different density. This model predicts no simple linear dependence on the amount of "extra" X-rays. If formation strengths are similar then a higher-density radial flow, which (dependent on its speed) would probably occur at higher luminosity, might suppress the QPOs more.

We would like to thank various participants of the 1999 workshop on X-ray Probes of Relativistic Astrophysics at the Aspen Center for Physics for pleasant and extremely fruitful discussions. We are specially grateful to Phil Kaaret, Fred Lamb, Coleman Miller, Dimitrios Psaltis, Luigi Stella, and Will Zhang. M. M. thanks the Max-Planck Institut für Astrophysik in Munich, for its hospitality during the completion of part of this work. This work was supported by the Netherlands Research School for Astronomy (NOVA), the Netherlands Organization for Scientific Research (NWO) under contract 614-51-002 and the NWO Spinoza grant 08-0 to E. P. J. van den Heuvel. M. M. is a fellow of the Consejo Nacional de Investigaciones Científicas y Técnicas de la República Argentina. This research has made use of data obtained through the High Energy Astrophysics Science Archive Research Center Online Service, provided by the NASA/Goddard Space Flight Center.

REFERENCES

Barret, D., Olive, J. F., Boirin, L., Grindlay, J. E., Bloser, P. F., Chou, Y., Swank, J. H., & Smale, A. P. 1997, IAU Circ. 6793
Berger, M., et al. 1996, ApJ, 469, L13
Bloser, P. F., Grindlay, J. E., Kaaret, P., Zhang, W., Smale, A. P., & Barret, D. 2000, ApJ, 542, 1000
Boirin, L., Barret, D., Olive, J. F., Grindlay, J. E., & Bloser, P. F. 2000, Adv. Space Res., 25, 387
Campana, S. 2000, ApJ, 534, L79
Cui, W. 2000, ApJ, 534, L31
Cui, W., Barret, D., Zhang, S. N., Chen, W., Boirin, L., & Swank, J. 1998, ApJ, 502, L49
Di Salvo, T., Méndez, M., van der Klis, M., Ford. E. C., & Robba, N. R. 2001, ApJ, 546, 1107
Fender, R. P., & Hendry, M. A. 2000, MNRAS, 317, 1
Ford, E., et al. 1997a, ApJ, 475, L123
———. 1997b, ApJ, 486, L47
Ford, E., & van der Klis, M. 1998, ApJ, 506, L39
Ford, E. C., van der Klis, M., Méndez, M., Wijnands, R., Homan, J., Jonker, P. G., & van Paradijs, J. 2000, ApJ, 537, 368
Fortner, B., Lamb, F. K., & Miller, G. S. 1989, Nature, 342, 775
Ghosh, P., & Lamb, F. K. 1979, ApJ, 234, 296
Hasinger, G., & van der Klis, M. 1989, A&A, 225, 79
Homan, J., & van der Klis, M. 2000, ApJ, 539, 847
Jonker, P. G., Wijnands, R., van der Klis, M., Psaltis, D., Kuulkers, E., & Lamb, F. K. 1998, ApJ, 499, L191
Jonker, P. G., et al. 2000, ApJ, 537, 374
Kaaret, P., Piraino, S., Bloser, P. F., Ford, E. C., Grindlay, J. E., Santangelo, A., Smale, A. P., & Zhang, W. 1999a, ApJ, 520, L37
Kaaret, P., Piraino, S., Ford, E. C., & Santangelo, A. 1999b, ApJ, 514, L31
Kaaret, P., Yu, W., Ford, E. C., & Zhang, N. S. 1998, ApJ, 497, L93
Lee, H. C., & Miller, G. S. 1998, MNRAS, 299, 479
Lehr, D. E., Wagoner, R. V., & Wilms, J. 2000, ApJ, submitted (astro-ph/0004211)
Markwardt, C. B., Strohmayer, T. E., & Swank, J. E. 1999, ApJ, 512, L125

Méndez, M. 2000, Proc. 19th Texas Symposium on Relativistic Astrophysics and Cosmology, ed. J. Paul, T. Montmerle, & E. Aubourg (Amsterdam: Elsevier), 15
———. 2001, in The Neutron Star Black Hole Connection, ed. C. Kouveliotou, J. van Paradijs, & J. Ventura (NATO ASI Ser), in press
Méndez, M., & van der Klis, M. 1999, ApJ, 517, L51
Méndez, M., van der Klis, M., Ford, E. C., Wijnands, R., & van Paradijs, J. 1999, ApJ, 511, L49
Méndez, M., van der Klis, & van Paradijs, J. 1998a, ApJ, 506, L117
Méndez, M., van der Klis, & van Paradijs, J., Lewin, W. H. G., Vaughn, B. A., & Kuulkers, E. 1998b, ApJ, 494, L65
Méndez, M., van der Klis, M., Wijnands, R., Ford, E. C., van Paradijs, J., & Vaughan, B. A. 1998c, ApJ, 505, L23
Miller, M. C., Lamb, F. K., & Psaltis, D. 1998, ApJ, 508, 791
Osherovich, V., & Titarchuk, L. 1999, ApJ, 522, L113
Psaltis, D., Belloni, T., & van der Klis, M. 1999b, ApJ, 520, 262
Reig, P., Méndez, M., van der Klis, M., & Ford, E. C. 2000, ApJ, 530, 916
Stella, L., & Vietri, M. 1998, ApJ, 492, L59
———. 1999, Phys. Rev. Lett., 82, 17
Strohmayer, T. E., Zhang, W., & Swank, J. H. 1997, ApJ, 487, L77
Strohmayer, T. E., Zhang, W., Swank, J. H., Smale, I., Titarchuk, L., Day, C., & Lee, U. 1996, ApJ, 469, L9
van der Klis, M. 1995, in X-ray Binaries, ed. W. H. G. Lewin, J. van Paradijs, & E. P. J. van den Heuvel (Cambridge: Cambridge Univ. Press), 252
van der Klis, M. 1997, in Astronomical Time Series, ed. D. Maoz et al. (Dordrecht: Kluwer), 218, 121
———. 2001, ApJ, submitted (astro-ph/0106291)
van der Klis, M., Hasinger, G., Damen, E., Penninx, W., van Paradijs, J., & Lewin, W. H. G. 1990, ApJ, 360, L19
van Straaten, S., Ford, E. C., van der Klis, M., Méndez, M., & Kaaret, P. 2000, ApJ, 540, 1049
Vaughan, B. A., et al. 1997, ApJ, 483, L115
———. 1998, ApJ, 509, L145
White, N. E., & Zhang, W. 1997, ApJ, 490, L87
Wijnands, R., Méndez, M., van der Klis, M., Psaltis, D., Kuulkers, E., & Lamb, F. K. 1998a, ApJ, 504, L35
Wijnands, R. A. D., van Der Klis, M., Psaltis, D., Lamb, F. K., Kuulkers, E., Dieters, S., van Paradijs, J., & Lewin, W. H. G. 1996, ApJ, 469, L5
Wijnands, R., et al. 1997, ApJ, 490, L157
———. 1998b, ApJ, 493, L87
Wijnands, R., & van der Klis, M. 1999, ApJ, 514, 939
Zhang, W., Jahoda, K., Kelley, R. L., Strohmayer, T. E., Swank, J. H., & Zhang, S. N. 1998, ApJ, 495, L9
Zhang, W., Strohmayer, T. E., & Swank, J. H. 1997, ApJ, 482, L167